

GRIBOV THEORY OF NUCLEAR INTERACTIONS AND PARTICLE DENSITIES  
AT FUTURE HEAVY-ION COLLIDERS .

A. Capella<sup>a)</sup>, A. Kaidalov<sup>a),b)</sup> and J. Tran Thanh Van<sup>a)</sup>

a) Laboratoire de Physique Théorique,

Unité Mixte de Recherche (CNRS) UMR 8627

Université de Paris XI, Bâtiment 210, F-91405 Orsay Cedex, France

b) ITEP, B.Chermushkinskaya 25, 117526 Moscow, Russia

**Abstract**

Gribov approach to high-energy interactions of hadrons and nuclei is reviewed and applied to calculation of particle production in heavy-ions collisions. It is pointed out that the AGK (Abramovsky, Gribov, Kancheli) cutting rules is a powerful tool to investigate particle spectra in these processes. It leads, in the Glauber approximation, to a simple formula for the density of hadrons produced in the central rapidity region in nucleus-nucleus interactions. An estimate of this density for RHIC and LHC is presented and compared with results of Monte-Carlo calculations. It is shown that the Glauber approximation substantially overestimate particle densities compared to the results of the complete Gribov theory. This is due to extra shadowing in the system, related to large mass diffraction which leads to a strong decrease of particle densities at mid rapidities. Our method of calculation of these effects has been applied to the problem of shadowing of nuclear structure functions and a good agreement with experimental data has been obtained.

Contributed paper to the  
*Gribov Memorial Volume*  
of Acta Physica Hungarica (Heavy Ion Physics).

LPT ORSAY 99-15

March 1999

arXiv:hep-ph/9903244v1 3 Mar 1999

# 1 Introduction

The reggeon approach to high-energy interactions is undoubtedly an important ingredient of modern theory. V.N. Gribov has made very essential contributions to the development of this approach. He has introduced a leading pole in the complex angular momentum plane [1], which determines asymptotics of diffractive processes (nowadays called the Pomeron), investigated the main properties of Regge-poles [2] and Regge-cuts [3] and developed the reggeon diagram technique [4].

An important contribution to the theory of multiparticle production has been made by V.N. Gribov together with V.A. Abramovsky and O.V. Kancheli [5] and is usually referred to as the AGK-cutting rules. These rules are widely used for the construction of QCD-based models for high-energy interactions (for reviews see [6, 7]). In this paper we will extensively use AGK-cutting rules and Gribov reggeon diagram technique to calculate inclusive particle spectra and particle densities in the central rapidity region for heavy-ions collisions at future colliders RHIC and LHC. The values of particle and energy densities are very important for the problem of creation of the quark-gluon plasma in heavy-ions collisions at these very high energies.

In the first part of the paper (Section 2) we will shortly review Gribov's approach to high-energy interactions of hadrons with nuclei [8] and note the difference in the space-time picture of interactions at low and high energies. We will also discuss a difference between the Glauber approximation and the general Gribov theory. The AGK-cutting rules will be applied to hadron-nucleus and nucleus-nucleus collisions and a simple formula for inclusive particle spectra and densities of produced particles in the central rapidity region valid in the Glauber approximation will be presented.

Applications of the Regge-Gribov theory to high-energy hadronic interactions are considered in Section 3. The important role of shadowing effects in these processes is emphasized. It is pointed out that understanding diffractive processes is important for a selfconsistent description of high-energy interactions of hadrons and nuclei. The results of this analysis are used in the Section 4 to estimate particle densities at RHIC and LHC. Limitations of the Glauber approximation and its modification at high energy according to the Gribov theory will be discussed. It will be shown that these modifications are related to large mass diffraction dissociation of hadrons which leads to extra shadowing in the system. These effects reduce particle densities in the central rapidity region compared to the Glauber approximation predictions. This result is valid for both soft and hard processes. To estimate these shadowing effects we apply Gribov theory to the processes of deep inelastic scattering (DIS) on nuclei and show how it is possible to calculate nuclear shadowing effects in the region of small Bjorken- $x$ , using information on diffractive production in DIS. Our results agree with existing experimental data and allow

a safe extrapolation of shadowing effects to the experimentally unmeasured region of very small  $x$ , relevant for nuclear collisions at LHC. This model leads to a reduction of particles densities in PbPb collisions at LHC (RHIC) by a factor of three (two), with respect to the results of the Glauber approximation. Our results are compared to predictions of different Monte–Carlo calculations.

## 2 Gribov theory of high-energy nuclear interactions

In classical papers of Gribov [8] it was shown how to incorporate the Glauber model [9] for interactions of hadrons with nuclei into a general framework of relativistic quantum theory. Consider an amplitude of elastic scattering for high–energy hadron–nucleus interactions. In the Glauber model it is described by the diagrams shown in Fig. 1, which looks like a successive rescatterings of initial hadron on nucleons of the nucleus. However, as was emphasized by Gribov [8, 10] the space–time picture of the interaction at high–energy  $E > m_h \mu R_A$  ( $\mu$  is a characteristic hadronic scale  $\sim 1 \text{ GeV}$  and  $R_A$  is the radius of the nucleus) is completely different from this simple picture. It corresponds to coherent interactions of a fluctuation of the initial hadron, which is “prepared” long before its interaction with the nucleus (Fig. 2). A very important result of Gribov [8] is that nevertheless the elastic  $hA$ –amplitude can be written as a sum of the diagrams shown in Fig. 3, with elastic rescatterings (Fig. 3a) which give the same result as Glauber model, plus all possible diffractive excitations of the initial hadron. At not too high energies  $E_L \sim 10^2 \text{ GeV}$  these terms lead to corrections to the Glauber approximation of 10 – 20% for the total  $hA$  cross section [11, 12].

We will show below that at very high energies and for inclusive cross sections this modification of the Glauber approximation is very important. The difference between Glauber model and Gribov’s theory is essential for understanding shadowing corrections for structure functions of nuclei related to hard processes on nuclei and for many aspects of multiparticle production on nuclei [13].

An important consequence of the space–time structure of the diagrams of Fig. 2 for interactions of hadrons with nuclei is the theorem, based on AGK–cutting rules [5], that for inclusive cross sections all rescatterings cancel with each other and these cross sections are determined by the diagrams shown in Fig. 4 (impulse approximation). Note, however, that this result, valid asymptotically in the central rapidity region, only applies to the diagrams of the Glauber–type, i.e. when masses of intermediate states in Fig. 3 are limited and do not increase with energy. As a result, the inclusive cross section for the production of a hadron  $a$  is expressed, for a given impact parameter  $b$ , in terms of inclusive cross section for  $hN$  interactions

$$E \frac{d^3 \sigma_{hA}^a(b)}{d^3 p} = T_A(b) E \frac{d^3 \sigma_{hN}^a}{d^3 p} \quad (1)$$

where  $T_A(b)$  is the nuclear profile function ( $\int d^2 b T_A(b) = A$ ). After integration over  $b$  we get

$$E \frac{d^3 \sigma_{hA}^a}{d^3 p} = A E \frac{d^3 \sigma_{hN}^a}{d^3 p} \quad (2)$$

The total and inelastic hA cross sections in the Glauber model can be easily calculated and are given for heavy nuclei by well known expressions. For example

$$\sigma_{hA}^{in} = \int d^2 b (1 - \exp(-\sigma_{hN}^{in} T_A(b))) \quad (3)$$

The situation for nucleus–nucleus collisions is much more complicated. There are no analytic expressions in the Glauber model for heavy–nuclei elastic scattering amplitudes. The problem stems from a complicated combinatorics and from the existence of dynamical correlations related to “loop diagrams” [14, 15]. Thus, usually optical–type approximation [16, 17] and probabilistic models for multiple rescatterings [18] are used. For inclusive cross sections in AB–collisions the result of the Glauber approximation is very simple to formulate due to the AGK cancellation theorem. It is possible to prove, for an arbitrary number of interactions of nucleons of both nuclei [19], that all rescatterings cancel in the same way as for hA–interactions and only the diagrams of Fig. 5 contribute to the single inclusive spectrum. Thus a natural generalization of eq. (1) for inclusive spectra of hadrons produced in the central rapidity region in nucleus–nucleus interactions takes place in the Glauber approximation

$$E \frac{d^3 \sigma_{AB}^a(b)}{d^3 p} = T_{AB}(b) E \frac{d^3 \sigma_{NN}^a}{d^3 p} \quad (4)$$

where  $T_{AB}(b) = \int d^2 s T_A(\vec{s}) T_B(\vec{b} - \vec{s})$ . After integration over  $b$  eq. (4) reads

$$E \frac{d^3 \sigma_{AB}^a}{d^3 p} = AB E \frac{d^3 \sigma_{NN}^a}{d^3 p} \quad (5)$$

Note that eqs.(4),(5) are valid for an arbitrary set of Glauber diagrams and are not influenced by the problem of summation of “loop” diagrams mentioned above.

The densities of charged particles can be obtained from eqs.(4), (5) by deviding them by the total inelastic cross section of nucleus–nucleus interaction. For example

$$\frac{dn_{AB}^{ch}(b)}{dy} = \frac{T_{AB}(b)}{\sigma_{AB}^{in}} \frac{d\sigma_{NN}^{ch}}{dy} \quad (6)$$

and

$$\frac{dn_{AB}^{ch}}{dy} = \frac{AB}{\sigma_{AB}^{in}} \frac{d\sigma_{NN}^{ch}}{dy} \quad (7)$$

In the following we shall use these results to calculate particle densities in the central rapidity region at energies of RHIC and LHC.

### 3 Regge-Gribov theory and hadronic interactions.

In this section we will briefly review results obtained as an application of the Gribov theory to hadronic interactions at very high energies. We will need them in order to determine inclusive particle spectra in NN-interactions at RHIC and LHC and in order to illustrate the importance of inelastic diffractive processes for a selfconsistent treatment of high-energy hadronic interactions.

In the traditional Gribov's reggeon approach it is assumed that the Pomeron is a Regge pole accompanied by the cuts associated to the multi-Pomeron exchanges in the  $t$ -channel. These cuts are important to restore the unitarity of the theory. Reggeon diagrammatic technique [4] and the AGK cutting rules [5] allow one to calculate contributions of many-Pomeron exchanges to scattering amplitudes and relate them to the properties of multiparticle production.

An important parameter of the theory is the value of the Pomeron intercept  $\alpha_P(0)$ . In the simplest model, where only the single-Pomeron exchange is taken into account the intercept determined from the analysis of  $\sigma^{tot}$  and elastic scattering data is  $\alpha_P(0) \approx 1.08$  [20]. However, this is only an effective value of the intercept  $\alpha_P^{eff}(0)$ , which describes the energy dependence of total hadronic cross sections in the currently available range of energies,  $\sigma^{(tot)} \sim s^{\alpha_P^{eff}(0)-1}$ . An extensive phenomenological analysis, which takes into account multi-Pomeron exchanges, (see e.g. refs. [6, 7]) shows that the Pomeron intercept is substantially larger than the value  $\alpha_P^{eff}(0)$  indicated above. With eikonal type diagrams only one gets  $\alpha_P(0) = 1.12 \div 1.15$  [21]. For a more complete set of diagrams, which include interactions between exchanged Pomerons (related to large mass diffractive production), an even larger intercept of  $\alpha_P(0) \approx 1.2$  is obtained [22].

In this approach many characteristics of high energy hadronic interactions are well described [6, 7]. Multi-Pomeron exchanges are very important for understanding many qualitative features of experimental data. For example the fast increase of inclusive spectra in the central rapidity region can be reproduced only if multi-chain configurations, which are due to cutting of multi-Pomeron diagrams, are taken into account. For pure pole model the density of produced hadrons in the central region would be energy independent at large  $s$ . Experimentally in pp-interactions it increases with energy approximately as  $s^\delta$  with  $\delta \approx 0.13$ .

Another manifestation of multipomeron exchanges is an existence of important long-range correlations (for example forward–backward correlations). They are firmly established experimentally at high energies. Long range correlations are closely related to broad multiplicity distributions. The models based on the reggeon diagrams technique and AGK–cutting rules give a good quantitative descriptions of multiplicity distributions including violation of the KNO–scaling at very high energies.

Let us consider now diffractive production of hadrons at very high energies. Description of these processes in the Regge–model can be found in reviews [23, 24, 25]. The differential cross section for inclusive single diffraction dissociation can be written in the form [23]

$$s_2 \frac{d^2\sigma}{ds_2 dt} = \frac{(g_{pp}^P(t))^2}{16\pi} |G_P(\xi', t)|^2 \sigma_{Pp}^{(tot)}(s_2, t) \quad (8)$$

where  $s_2 = M^2$ ,  $M$  is an invariant mass of the produced state,  $G_P(\xi', t) = \eta(\alpha_P(t)) \exp[(\alpha_P(t) - 1)\xi]$ ,  $\xi = \ln(s/s_2)$  and  $\eta(\alpha_P(t))$  is the signature factor. The quantity  $\sigma_{Pp}^{tot}(s_2, t)$  is the total cross section for Pomeron–particle interaction. This cross section has asymptotic Regge behavior for large mass values of  $s_2$  - the squared of diffractively produced state. In this case, the cross section for diffraction dissociation is described by the triple–Regge diagrams (Fig. 6) and has the form

$$\begin{aligned} s_2 \frac{d^2\sigma}{ds_2 dt} &= \frac{(g_{pp}^P(t))^2}{16\pi} |G_P(\xi, t)|^2 \sum_k g_{pp}^k(0) r_{PP}^{\alpha_k} \left(\frac{s_2}{s_0}\right)^{\alpha_k(0)-1} \\ E \frac{d^3\sigma}{d^3p} &= \sum_k G_k(t) \left(\frac{s_2}{s}\right)^{\alpha_k(0)-2\alpha_P(t)} \left(\frac{s}{s_0}\right)^{\alpha_k(0)-1} \end{aligned} \quad (9)$$

Values of  $\sigma_{Pp}^{(tot)}(s_2, t)$  and of the triple reggeon vertices  $r_{PP}^P, r_{PP}^f$  have been determined from analyses of diffractive production in hadronic collisions [6, 24, 25, 26].

In the pole approximation with  $\Delta = 0.08$  the total cross section of inelastic diffraction increases too fast with energy and strongly contradicts to experimental data at  $\sqrt{s} \sim 10^3 \text{ GeV}$ . This problem is solved by the inclusion of Regge cuts. For example in ref. [22] a much slower increase of  $\sigma_D$ , consistent with recent experimental result, was predicted even for  $\Delta = 0.21$ . It is important to note that in Gribov theory the amount of shadowing is closely related to the magnitude of diffractive processes, which in their turn are influenced by the shadowing. This complicated, nonlinear problem can be solved only by a systematic and selfconsistent treatment of both diffractive processes (elastic and inelastic) and multiparticle production.

## 4 Particle densities in heavy–ions collisions at super-high energies

Now we will address the question of particle densities in heavy–ions collisions at energies of future colliders. For central PbPb collisions at LHC ( $\sqrt{s} \sim 6$  TeV), existing Monte-Carlo models (see [27]) give a rather broad range of values, of  $dn^{ch}/dy$  at  $y^* \sim 0$  –from about 8000 particles for the VENUS model [28] to  $\approx 1400$  particles for the String Fusion Model (SFM) [29]. Other Monte–Carlo models [30, 31] give predictions within this interval. All these models are based on the probabilistic approximation to the Glauber model of nuclear interactions and should lead to similar results for inclusive particle densities, which according to eqs.(6)-(7), do not depend on details of the particular model (for NN-interactions all these models give similar predictions, since the extrapolation from the experimentally measured region of energies is not large). Below, we shall compare these results of Monte–Carlo models and of semi–analytic calculations [32] with predictions of eqs.(6),(7) and shall discuss deviations from the Glauber approximation build in some of these models. Finally, we will compare them with predictions of the complete Gribov theory of nuclear collisions –i.e. including shadowing corrections due to high mass intermediate states in Fig. 3.

Eq. (7) for particle densities integrated over impact parameter (minimum bias events) can be rewritten as

$$\frac{dn_{AB}^{ch}}{dy} = n_{AB} \frac{dn_{NN}^{ch}}{dy} \quad (10)$$

where  $n_{AB} = \frac{AB\sigma_{NN}^{in}}{\sigma_{AB}^{in}}$ . It corresponds to the average number of collisions in the Glauber model. For  $A = B \gg 1$   $n_{AB}$  behaves as  $CA^{4/3}$  with  $C \approx \frac{\sigma_{NN}^{in}}{4\pi R_0^2}$  ( $R_A = R_0 A^{1/3}$ ). It is well known that eqs.(4),(5),(10) can be applied to hard processes but in the Glauber approximation they are valid for soft processes as well. We shall see below that for both soft and hard processes these equations have to be modified.

For characteristics of pp–interaction at  $\sqrt{s} = 6$  TeV we take predictions of the Quark–Gluon String model [6] and dual parton model (DPM) [6, 7] : total inelastic cross section  $\sigma_{pp}^{in} = 65$  mb, inelastic nondiffractive cross section  $\sigma_{pp}^{in,nonD} = 50$  mb, and for density of charged particles at  $y = 0$  for nondiffractive interactions  $dn_{pp}^{ch}/dy = 5.0$ . The uncertainty in these numbers is  $\approx 10\%$ . The total inelastic cross section for nucleus–nucleus collisions can be calculated either using a simple geometrical formula or the optical approximation to Glauber model, which both give at LHC energies for PbPb collisions a value  $\approx 5$  barn (in these estimates an increase of the radius of NN–interaction with energy has been taken into account). Using these numbers and eqs.(7),(10) we obtain for PbPb collisions at LHC at  $y^* = 0$  the following numbers for minimum bias events and central ( $b < 3$  fm)

collisions, respectively

$$dn^{ch}/dy = 2100 \quad , \quad dn^{ch}/dy = 8500 \quad . \quad (11)$$

These numbers are close to results of the VENUS model [28] and to the DPM results of ref. [32] (1890 and 7900 respectively, with a slightly different definition of central collisions). However, the results of SFM [29] without string fusion and DPMJET-II [31] are about twice smaller. For SFM this can be due to the fact that this code has limits on the number of produced strings and is not reliable at LHC energies [33].

Thus, the Glauber approximation predicts very large densities of charged hadrons in central heavy-ions collisions at LHC. However, are these predictions realistic ? In order to answer this question we will consider possible limitations of the Glauber approximation and also the corrections to the AGK cancellation theorem which are important at high energies.

There are two types of corrections to eqs.(1),(4),

a) The effects due to energy-momentum conservation [34], –the energy of the initial hadron is shared by "constituents" (see Fig. 2) and each sub-collision happens at smaller energy. These effects are very important in the fragmentation regions of colliding hadrons (or nuclei) and reduce particle densities. For  $y^* = 0$  this reduction decreases as  $(1/s)^{1/4}$ . It is important at SPS energies ; however, at LHC energies in the central rapidity region this effect is small. It is taken into account in the Monte-Carlo models mentioned above.

b) Another dynamical effect is important at very high energies when diffractive production of very heavy hadronic states ( $M^2 \gg m_N^2$ ) becomes possible and should be taken into account in the diagrams of Fig. 3. Consider for example a double rescattering diagram of a proton on a nucleus, which contains, according to Gribov theory, the diffractive large-mass intermediate states shown in Fig. 7. It is related to the triple-Pomeron interaction discussed above and corresponds to an interaction between Pomerons (strings in the string models of particle production). As the total and inelastic cross sections of hA and AB-interactions at high energies are close to a black disc limit due to Glauber-type diagrams, these extra interactions have a small influence on total cross sections. However, they are very important for inclusive spectra in the central rapidity region [13], where contributions of Glauber rescatterings cancel due to AGK rules.

The diagram shown in Fig. 7 is only one of a large class of diagrams with interactions between Pomerons. The application of AGK-cutting rules to these diagrams leads to the diagrams for inclusive cross section in AB-collisions shown in Fig. 8. Extra shadowing effects related to these diagrams modify the A-dependence of the Glauber approximation for inclusive spectra eqs.(1),(4) in such a way that the behaviour  $d\sigma_{AB}/dy \sim AB$  of the Glauber approximation changes to  $d\sigma_{AB}/dy \sim A^\alpha B^\alpha$ , where  $\alpha < 1$ . For very strong interaction between Pomerons  $\alpha \rightarrow 2/3$  . This limit was considered by O.V. Kancheli a



long time ago [35]. It leads to universal particle densities in pp, pA and AB–collisions. We will show that due to a rather weak interaction between Pomerons even at LHC energies the value of  $\alpha$  is close to 0.9.

The problem of shadowing for inclusive spectra is not especially related to soft processes. The same graphs of Fig. 8 are relevant also for hard processes (production of jets or particles with large  $p_T$ , heavy quarks, large–mass lepton pairs, e t.c.). For hard processes, due to the QCD–factorization theorem, inclusive spectra in nucleus–nucleus collisions are given by convolutions of hard cross sections with distributions of partons in the colliding nuclei. In these cases the diagrams of Fig. 8 describe shadowing effects for nuclear structure functions (i.e. distributions of quarks and gluons in nuclei). Due to a coherence condition these effects are important only in the region of very small  $x_i$  of partons ( $x_i \ll 1/(R_A m_N)$ ). So these effects are important only at very high energies, when  $x_i \approx M_T/\sqrt{s}$  satisfy this condition. This condition in terms of  $x_i$  of partons coincides with the condition on diffractive production of large–mass states discussed above (see for example [36]).

The effects of shadowing are observed experimentally in deep inelastic scattering on nuclei [37, 38]. So in order to test the Gribov method of calculations of shadowing corrections we will apply it to these processes (Fig. 9). The first diagram in Fig. 9 corresponds to a sum of interactions with nucleons of nuclei and is proportional to  $A$ . The second diagram (Fig. 9b)) describes the shadowing effect due to a coherent interaction of a virtual photon with two nucleons of the nucleus and is related to diffractive production in DIS. This process was measured at HERA [39, 40] and was well described in the model, based on the triple–Regge diagrams of Fig. 10 [41, 42]. The study of diffraction dissociation of a virtual photon at HERA allows a better determination of triple–Regge couplings compared to hadronic reactions. This is related to the fact that diffraction dissociation in DIS is much less influenced by absorptive corrections than diffractive production in hadronic interactions, where “effective” vertices are much smaller than their “bare” values (see below, after eq. (17)).

The contribution of a double rescattering term to the  $\sigma_{\gamma^*p}$  is directly expressed in terms of the differential cross section for the diffraction dissociation of a virtual photon in  $\gamma^*N$ –interactions:

$$\sigma^{(2)} = -4\pi \int d^2b T_A^2(b) \int dM^2 \frac{d\sigma_{\gamma^*N}^{DD}(t=0)}{dM^2 dt} F_A(t_{min}) \quad (12)$$

where  $F_A(t_{min}) = \exp(R_A^2 t_{min}/3)$ ;  $t_{min} \approx -m_N^2 x_P^2$ .

Higher order rescatterings are model dependent and in the generalized Schwimmer model [43] we obtain for the ratio  $F_{2A}/F_{2N}$  structure functions  $F_2$  nuclei and nucleons, in the region of small  $x$

$$F_{2A}/F_{2N} = \int d^2b \frac{T(b)}{1 + F(x, Q^2)T(b)} \quad (13)$$

with  $F(x, Q^2) = 4\pi \int dM^2 \left( d\sigma_{\gamma^*N}^{DD}(t=0)/dM^2 dt \right) (F_A(t_{min})/\sigma_{\gamma^*N}(x, Q^2))$ .

Theoretical predictions [44] for nuclear shadowing based on the model for diffraction dissociation of ref. [42] are in a good agreement with NMC-data on nuclear structure functions at very small  $x$  [37], including very accurate data on Sn target (Fig. 11). The model describes both the  $x$  and  $Q^2$ -dependence of structure functions of nuclei and allows us to obtain reliable predictions for structure functions of nuclei in the region of  $x < 10^{-3}$  (Fig. 12) relevant for nuclear interactions at LHC energies. Let us mention at this point that while the distributions of quarks in nuclei are known experimentally and can be rather safely calculated in the experimentally unmeasured region of  $x$  and  $Q^2$ , the situation with gluons is much less clear. This problem is related to the distribution of gluons in the Pomeron, which can be in principle extracted from experimental data on diffractive production of jets or heavy-quarks in DIS. However, existing experimental data do not allow a reliable determination of this contribution. The terms with triple-Pomeron interaction, shown in Figs. 8,10 lead to a universal shadowing. So in the following we will assume that the shadowing effects at very small  $x$  are the same for quarks and gluons (the same assumptions was made in refs. [30, 45] while in some papers [46, 47] it is assumed that, due to a larger  $ggg$ -coupling compared to  $qqg$ -coupling, the shadowing for gluons is larger than for quarks).

The sum of diagrams of Fig. 5 and Fig. 8 leads to the following expression for inclusive spectra in nucleus-nucleus interactions.

$$E \frac{d^3\sigma_{AB}^a}{d^3p}(b) = \int d^2s f_A(\vec{b}) f_B(\vec{s} - \vec{b}) E \frac{d^3\sigma_{NN}^a}{d^3p} \quad (14)$$

where, in the Shwimmer model, the function  $f_A(b)$  coincides with  $\frac{T_A(b)}{1+F(x)T_A(b)}$  introduced above in the calculation of shadowing for nuclear structure functions. After integration over impact parameter  $b$  eq. (14) becomes

$$E \frac{d^3\sigma_{AB}^a}{d^3p} = F_A(s_A) F_B(s_B) E \frac{d^3\sigma_{NN}^a}{d^3p} \quad (15)$$

Where function  $F_A$  is the same as  $F_{2A}/F_{2N}$  defined above and is equal to  $A$  when the triple-Pomeron interactions is switched off. At  $y^* = 0$ ,  $s_A = s_B = m_T^a \sqrt{s}$  (which corresponds to  $x_i = m_T^a/\sqrt{s}$ ).

Thus, due to interactions between Pomerons, the Glauber formula (11) is modified in a simple way

$$\frac{dn_{AB}^{ch}}{dy} = \frac{dn_{AB, Glauber}^{ch}}{dy} \gamma_A \gamma_B \quad (16)$$

where the quantity  $\frac{dn_{AB,Glauber}^{ch}}{dy}$  is the Glauber approximation result –(eq. (10)) and  $\gamma_A$  is the shadowing correction to nuclear structure function  $F_{2A}/AF_{2N}$  shown in Fig. 12. In the following, we will consider it at a low scale  $Q^2 \sim 1 \text{ GeV}^2$  relevant to our problem. For LHC energies  $\gamma_{Pb} \approx 0.5 - 0.6$  and the total correction to the Glauber approximation for PbPb–collisions is  $0.25 \div 0.36$ . Formula (16) is written for minimum bias collisions. The result for different values of impact parameter  $b$  can be calculated using eq. (14). The calculation shows that for central collisions this correction differs by less than 10% from the value indicated above. Thus there is a suppression by a factor of  $\approx 3$  for charged particle densities at LHC energies compared to the results of the Glauber approximation given in (11). For PbPb–collisions at RHIC, particle densities are reduced by a factor  $\approx 2$  compared to the DPM predictions [32], which do not include shadowing corrections. However, in this case there are large uncertainties in the calculations of these corrections due to a strong dependence of the quantities  $\gamma_A$  on  $x_i$  in the region of  $x_i \sim 10^{-2}$ , relevant for these energies.

Let us emphasize that although our derivation of the shadowing corrections is based on the study of nuclear structure functions, which is valid for hard processes, we do not assume that hard processes dominate particle production at LHC–energies. In fact, the shadowing corrections due to triple–Pomeron interactions are universal and the same correction factors in eq. (16) are also obtained for soft interactions by a direct calculation of the diagrams of Fig. 8. In the Shwimmer model we will obtain the same expression  $\frac{T_A(b)}{1+F(s,y)T_A(b)}$  for shadowing where the function  $F(s, y)$  can again be written as an integral of the ratio of the triple Pomeron cross-section, eq. (9), over the single Pomeron exchange cross-section  $\sigma_P(y)$  :

$$\begin{aligned}
F(s, y) &= 4\pi \int_{y_{min}}^{y_{max}} dy \frac{1}{\sigma_P(y)} \left. \frac{d^2\sigma^{PPP}}{dy dt} \right|_{t=0} = \frac{(g_{pp}^P(0))^2 e}{4} \int_{y_{min}}^{y_{max}} d\xi \exp(\Delta\xi) = \\
&= \frac{(g_{pp}^P(0))^2 e}{4\Delta} [\exp(\Delta y_{max}) - \exp(\Delta y_{min})]
\end{aligned} \tag{17}$$

where  $y_{max} = y_{c.m.}^a + \frac{1}{2}\ell n(s/m_N^2)$ ,  $y_{min} = \ell n(R_A m_N)$ . We use the same parameters as in ref. [42] :  $(g_{pp}^P(0))^2 = 23 \text{ mb}$  is the Pomeron–proton coupling,  $\Delta \equiv \alpha_P(0) - 1 = 0.13$ ,  $e = r_{PPP}(0)/g_{pp}^P(0) \approx 0.07$ . Eq. (17) leads then to practically the same suppression factors as given above. Note that we are using here the same value of the triple Pomeron coupling as in DIS calculations [42]. As explained there, this value is about three times larger than the one obtained from a fit of soft hadronic diffraction using only triple Regge terms (without eikonal unitarization) as in refs. [6, 24, 25]. Such a large value of the triple Pomeron coupling is required in order to describe diffraction in DIS. In ref. [42], this was justified from the work of ref. [26], where it has been shown that eikonalization of  $\sigma_{SD}$

reduces its value by a factor close to 3 – implying that the true (or bare) triple Pomeron coupling is about 3 times larger than the effective one. In DIS, the eikonal corrections disappear very fast when  $Q$  increases and thus the bare coupling is the relevant one. In single particle inclusive production at high energies, the same is true since the eikonal corrections are absent due to the AGK cancellation. This is the physical reason for the large shadowing corrections obtained in this paper.

For collisions of identical nuclei (SS, PbPb) the  $A^{4/3}$ –dependence of particle densities of eq. (10) typical for the Glauber model changes to the behaviour  $A^\delta$ . The value of delta is a weak function of energy and it is equal to  $\delta \approx 1.1$  at LHC energies. It means that at these energies the values of  $\alpha$  in the A–dependence of inclusive cross sections for AB–collisions  $d\sigma_{AB}/dy \sim A^\alpha B^\alpha$  is close to 0.88. The value of  $\alpha$  should slowly decrease as energy increases. In the case of stronger shadowing for gluons than for quarks a somewhat smaller value of  $\alpha$  can be obtained.

Let us compare our results with Monte–Carlo calculations, which take into account shadowing effects [29, 30]. In the SFM model [29] the interaction between Pomerons is introduced via a mechanism of string fusion and is estimated from geometrical sizes of strings. The accuracy of such an estimate is not clear but it leads to a reasonable suppression factor (about 2) for particle densities at LHC energies (though application of the SFM Monte–Carlo is questionable at LHC ,–see above). In the Hijing model [30], existing data on nuclear shadowing were parameterized and thus the shadowing effects are also not very different from our predictions, though the Hijing model leads to a somewhat smaller suppression. This is connected to the choice of a saturation for shadowing at small values of  $x$  ( $x \sim 10^{-3}$ ) in their parameterization. The reggeon formalism allows us to determine the  $x$ –dependence of shadowing at small  $x$  and it shows that the shadowing is still increasing as  $x$  decreases even for  $x \sim 10^{-4}$ . Saturation happens at much smaller values of  $x$ .

## 5 Conclusions

Gribov theory of high–energy interactions of hadrons and nuclei is based on general properties of amplitudes in relativistic quantum theory and provides an unified approach to a broad class of processes. In this theory, the Glauber approximation to nuclear dynamics is valid in the region of not too high energies and should be modified at energies of RHIC and LHC. AGK– cutting rules provide a very powerful tool for the study of multiparticle production for all types of high–energy processes and allow one to obtain simple predictions for inclusive cross sections in hh, hA and AB–collisions.

In this paper we used AGK–cutting rules to obtain predictions for densities of particles

at future heavy–ions colliders. Gribov theory then allows to determine corrections to the Glauber approximation for inclusive particle spectra by relating them to cross sections of large–mass diffraction. The technique has been applied to calculation of shadowing effects for structure functions of nuclei and a good agreement with experimental data on these processes has been obtained. The same approach predicts a strong reduction of particle densities at super–high energies as compared to predictions of the Glauber approximation. Our calculations show that the DPM results [32] for PbPb collisions are reduced by a factor 3 at LHC and 2 at RHIC energies. The expected values of the charged particle density in central PbPb collisions at  $y^* = 0$  is thus 2500 at LHC and 1000 at RHIC.

Future experiments at RHIC and LHC will test these theoretical predictions and will allow a better determination of the parameters that govern the dynamics of shadowing.

### **Acknowledgments**

This work was supported in part by INTAS grant 93-0079ext., NATO grant OTR.LG 971390, RFBR grants 96-02-191184a, 96-15-96740 and 98-02-17463 .

## References

- [1] V.N. Gribov, JETP **41**, 667 (1961) (Sov. Phys. JETP **14**, 47 (1962) ).
- [2] V.N. Gribov, JETP **41**, 1962 (1961) (Sov. Phys. JETP **14**, 1395 (1962)).  
V.N. Gribov, I.Ya. Pomeranchuk, Phys. Rev. Lett. **2**, 232 (1962); JETP **43**, 1556 (1962)
- [3] V.N. Gribov, I.Ya. Pomeranchuk and K.A. Ter-Martirosyan, Phys. Rev. **B139**, 184 (1965).
- [4] V.N. Gribov, JETP **57**, 654 (1967) .
- [5] V.A. Abramovsky, V.N. Gribov and O.V. Kancheli, Sov. J. Nucl. Phys. **18**, 308 (1974).
- [6] A. Kaidalov, in “QCD at 200 TeV”, edited by L. Cifarelli and Yu. Dokshitzer, Plenum Press (1992) p.1 .
- [7] A. Capella, U. Sukhatme, C.-I. Tan and Tran Thanh Van, Phys. Rep. **236**, 225 (1994).
- [8] V.N. Gribov, JETP **56**, 892 (1969);  
V.N. Gribov, JETP **57**, 1306 (1969).
- [9] R.J. Glauber, Lectures in Theoretical Physics. Ed. Britten W.E. N.Y.: Int.Publ. 1959,v.1,p.315.
- [10] V.N. Gribov, Lectures at VII LIYAF Winter School of Physics, 1973,v.II,p.5.
- [11] A.B. Kaidalov, L.A. Kondratyuk, JETP Letters **15**, 170 (1972); Nucl. Phys. **B56**, 90 (1973).
- [12] V.V. Anisovich, L.G. Dakhno, P.E. Volkovitsky, Yad.Fiz. **15**, 168 (1972).
- [13] A.B. Kaidalov, Proc Quark Matter 90, Nucl. Phys. **A552**, 39c (1991).
- [14] I.V. Andreev, A.V. Chernov, Yad. Fiz. **28**, 477 (1978).
- [15] K.G. Boreskov, A.B. Kaidalov, Yad. Fiz. **48**, 575 (1988).
- [16] J. Formanek, Nucl. Phys. **B12**, 441 (1969).
- [17] W.Czyz and L.C. Maximon, Ann. Phys. (N.Y.) **52**, 59 (1969).

- [18] C. Pajares and A. V. Ramallo, Phys. Rev. **D31**, 2800 (1985).
- [19] K.G. Boreskov, A.B. Kaidalov, Acta Phys. Polon. **B20**, 397 (1989).
- [20] A. Donnachie, P.V. Landshoff, Phys. Lett. **B296**, 227 (1992).
- [21] A. Capella, J. Kaplan and J. Tran Thanh Van, Nucl. Phys. **B97**, 494 (1975).
- [22] A.B. Kaidalov, L.A. Ponomarev and K.A. Ter-Martirosyan, Sov.J.Nucl.Phys.**44**, 486 (1986).
- [23] A.B. Kaidalov, Phys. Rep. **50**, 157 (1979).
- [24] G. Alberi and G. Goggi, Phys. Rep. **74**, 1 (1981) .
- [25] K. Goulianos, Phys. Rep. **101**, 169 (1983).
- [26] A. Capella, J. Kaplan and J. Tran Thanh Van, Nucl Phys. **B105**, 333 (1976).
- [27] N. van Eijndhoven et al. The Alice Event Generator Pool, ALICE/GEN 95-32, Internal Note.
- [28] K. Werner , Phys. Rep. **232**, 87 (1993).
- [29] N.S. Amelin, M.A. Braun, C. Pajares, Z. Phys. **C63**, 507 (1994).
- [30] M. Gyulassy and X.N. Wang, Phys. Rev. **D44**, 3501 (1991).
- [31] J.Ranft et al., Phys. Rev. **D51**, 64 (1995).
- [32] A.Capella, C. Merino and J. Tran Thanh Van, Phys. Lett. **B265**, 415 (1991).
- [33] N. S. Amelin and E. G. Ferreira (private communications).
- [34] A. Capella, A.B. Kaidalov, Nucl. Phys. **B111**, 477 (1976).
- [35] O.V. Kancheli, Pisma v JETP **18**, 465 (1973).
- [36] K.G. Boreskov, A. Capella, A.B. Kaidalov and J. Tran Thanh Van, Phys. Rev. **D47**, 919 (1993).
- [37] P. Amaudruz et al. (NMC Collaboration), Nucl. Phys. **B441**, 3 (1995); M. Arneodo et al. (NMC Collaboration), Nucl. Phys. **B441**, 12 (1995); ibid. **B481** 3 (1996); ibid. **B481**, 23 (1996).
- [38] M.R. Adams et al. (E665 Collaboration), Phys. Rev. Lett. **68**, 3266 (1992); Zeit. Phys. **C67**, 403 (1995).

- [39] T. Ahmed et al. (H1 Collaboration), Nucl. Phys. **B429**, 477 (1994), Phys. Lett. **B348**, 681 (1995), Preprint DESY 97-158.
- [40] M. Derrick et al. (Zeus Collaboration), Zeit. Phys. **C68**, 569 (1995).
- [41] A. Capella, A. Kaidalov, C. Merino and J. Tran Than Van, Phys. Lett. **B343**, 403 (1995).
- [42] A. Capella, A. Kaidalov, C. Merino, D. Perterman and J. Tran Thanh Van, Phys. Rev. **D53**, 2309 (1996).
- [43] A. Schwimmer, Nucl. Phys. **B94**, 445 (1975).
- [44] A. Capella, A. Kaidalov, C. Merino, D. Perterman and J. Tran Thanh Van, Eur. Phys. Journ., **C5**, 111 (1998).
- [45] K.J. Eskola, V.J. Kolhinen and C.A. Salgado, JYFL-8/98, hep-ph/9807297.
- [46] Z. Huang, H.J. Lu and I. Sarcevic, Nucl. Phys. **A637**, 79 (1998)
- [47] H. Hammon, H. Stocker, W. Greiner, hep-ph/9811242.



## FIGURE CAPTIONS

**Fig. 1** Diagrams of the Glauber model for the elastic  $hA$ -scattering amplitude.

**Fig. 2** Diagrams for high-energy  $hA$ -interactions.

**Fig. 3** The dispersion representation diagrams for  $hA$ -elastic scattering amplitude. A cross on a line means that the particle is on the mass shell.

**Fig. 4** The diagram for inclusive cross section of particle  $a$  in  $hA$ -collisions.

**Fig. 5** The diagram for inclusive cross section in the Glauber approximation for AB-collisions.

**Fig. 6** Triple-regge diagrams for diffractive production of large-mass states in  $pp$ -collisions.

**Fig. 7** Large-mass diffractive contribution to  $pA$ -elastic scattering amplitude.

**Fig. 8** Diagrams for inclusive cross sections in AB-collisions, which take into account interactions between Pomerons.

**Fig. 9** Diagrams for  $\gamma^*A$  interactions.

**Fig. 10** Triple-regge diagrams for diffractive production in  $\gamma^*p$ -interactions.

**Fig. 11** The ratios  $\frac{A_1 F_2^{A_1}}{A_2 F_2^{A_2}}$ . Experimental points are from ref. [37].

**Fig. 12** The ratios  $F_2^A/AF_{2N}$  computed from eq. (13).

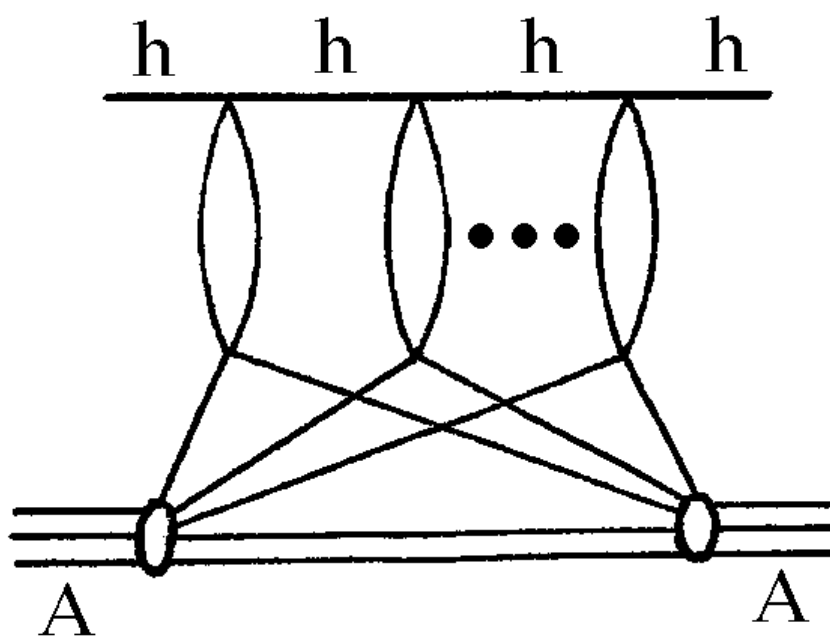


Fig. 1

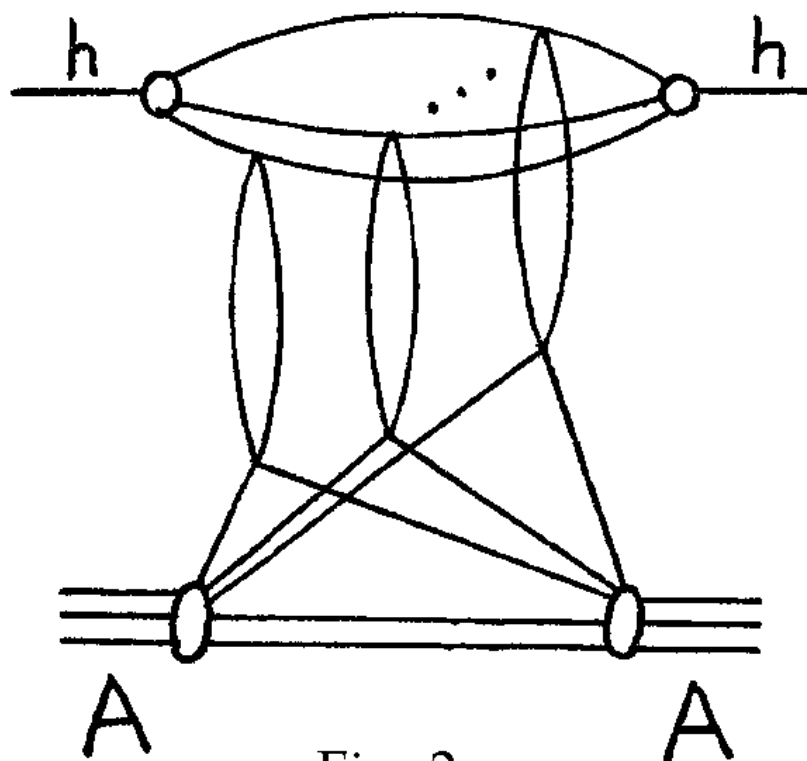


Fig. 2

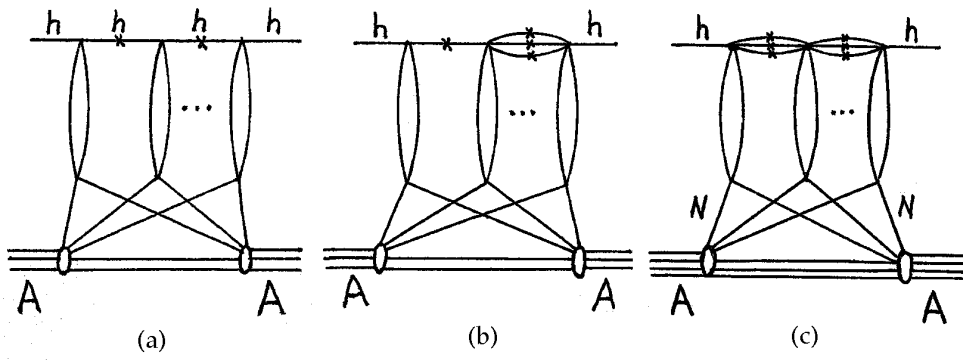


Fig. 3

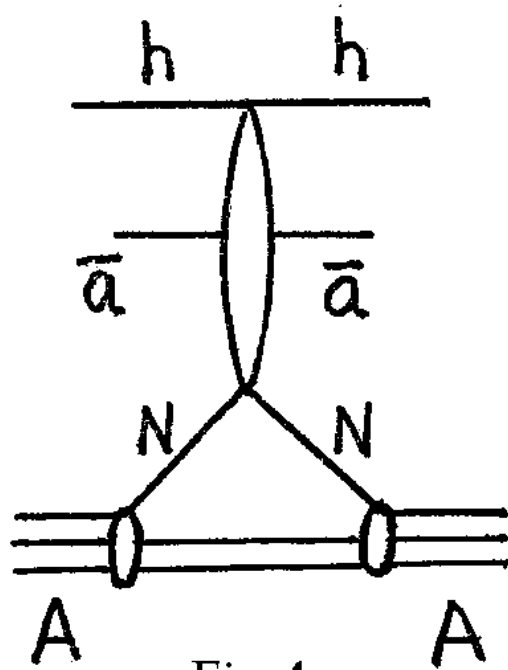


Fig 4

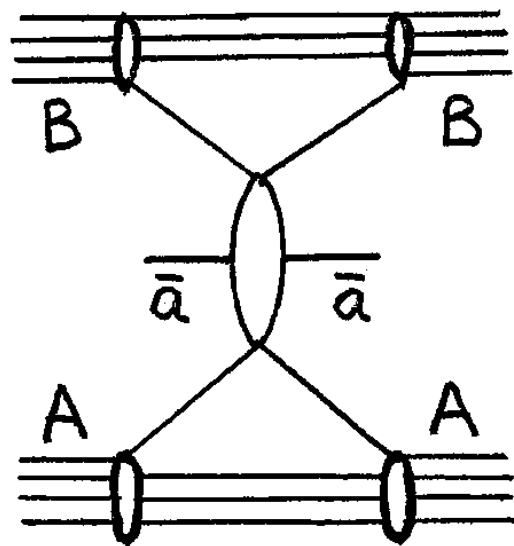


Fig 5

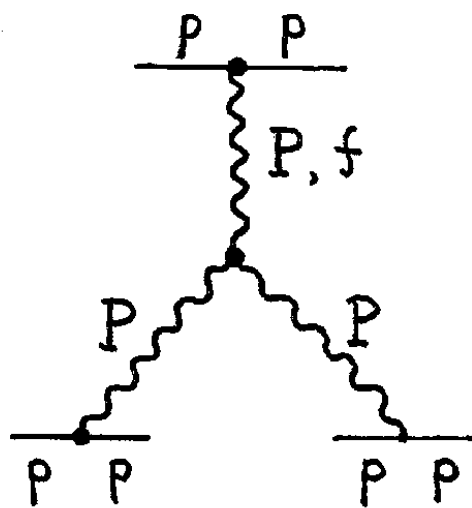


Fig 6

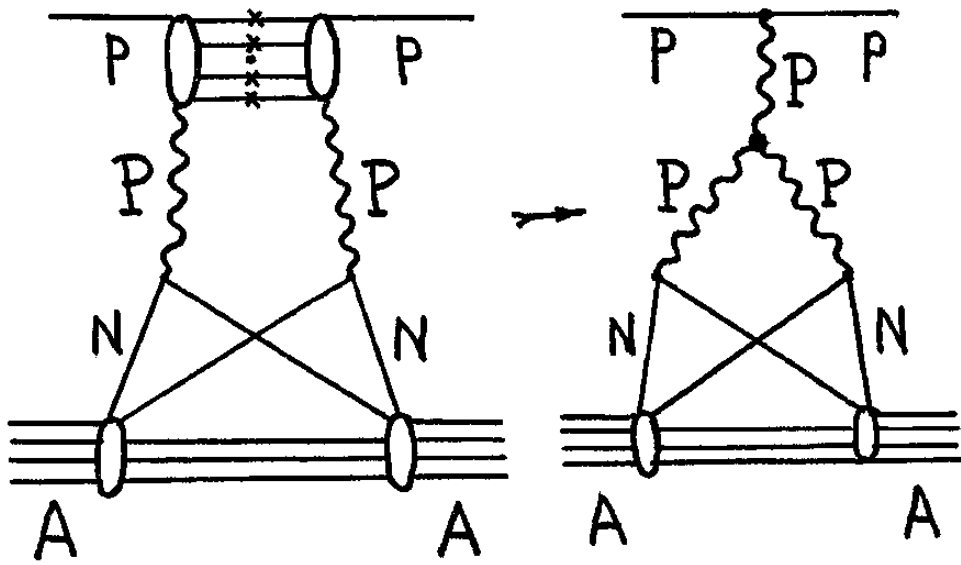


Fig 7

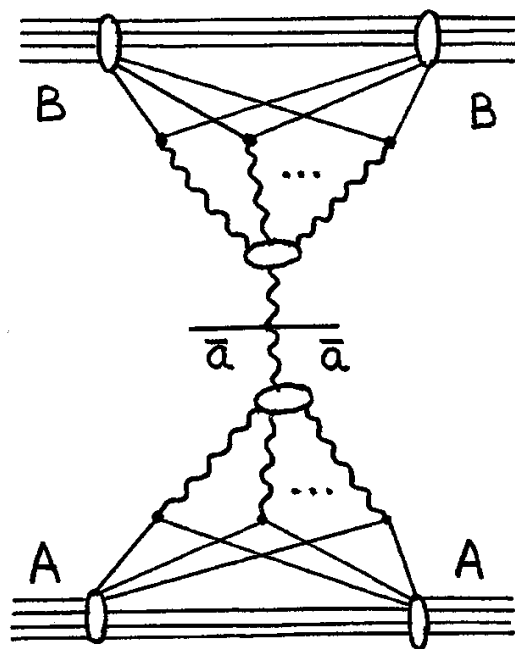


Fig 8

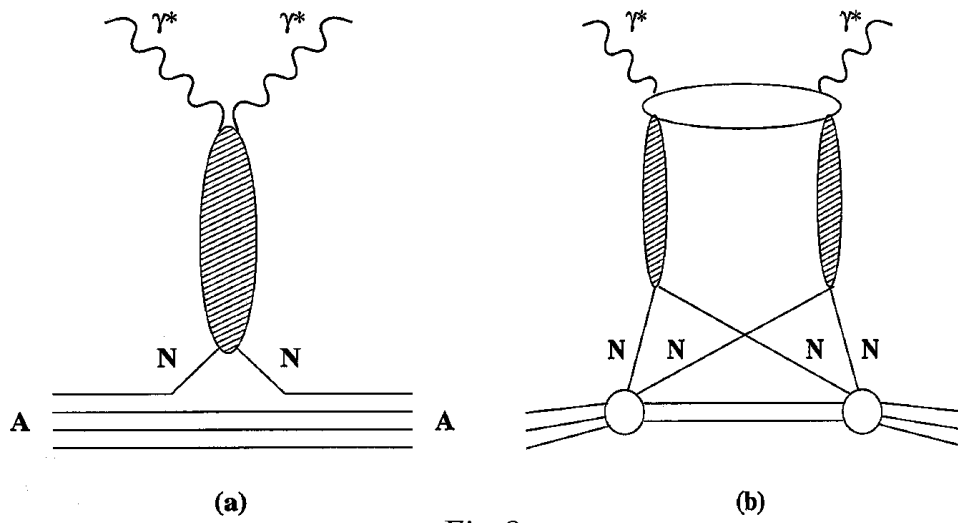


Fig 9

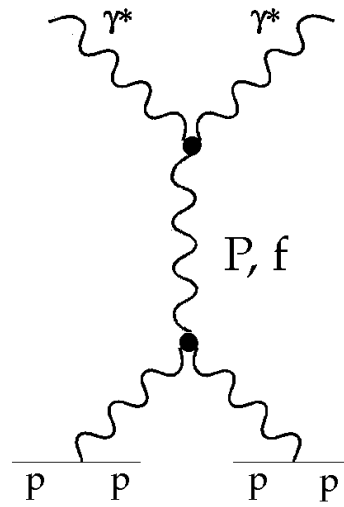


Fig 10

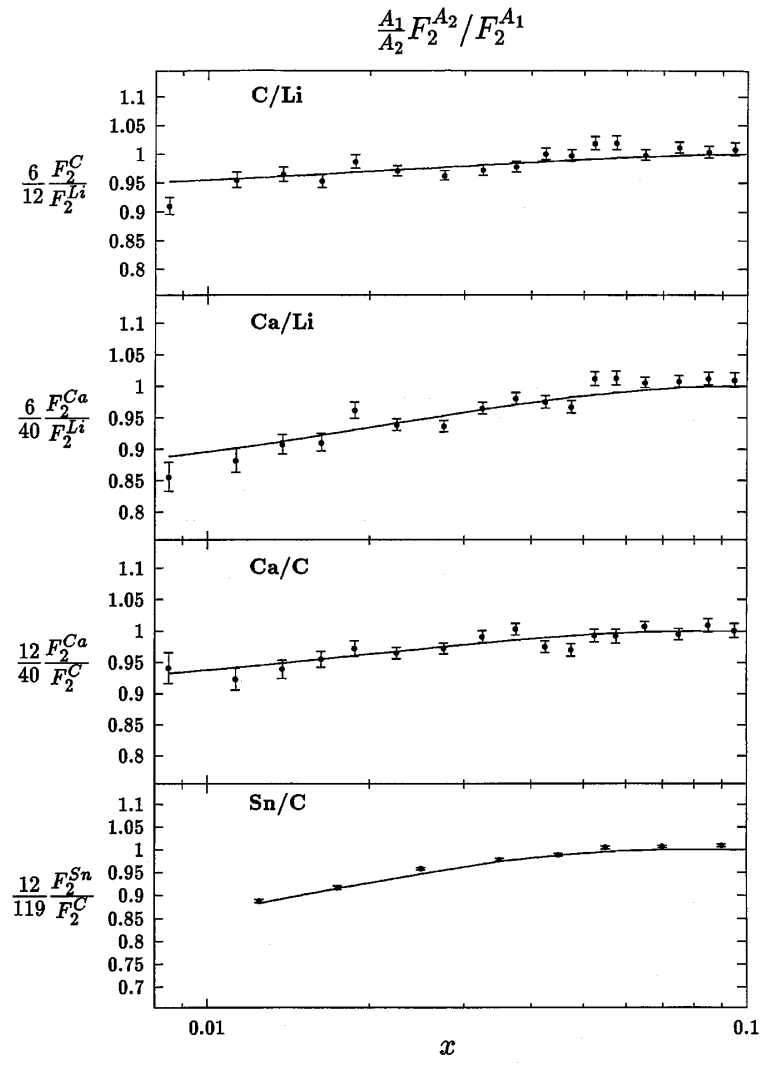


Fig. 11

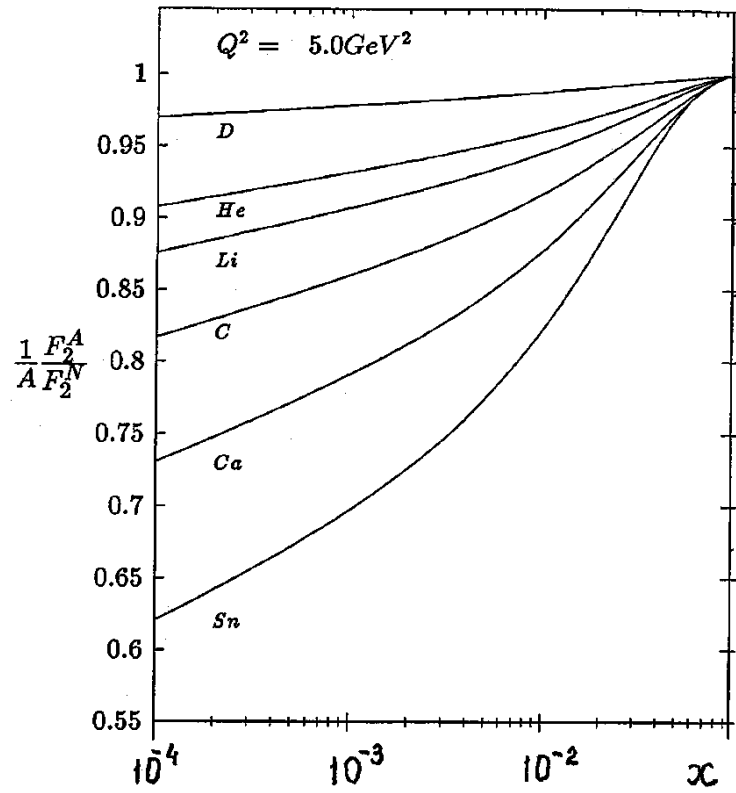


Fig 12